BioscienceHorizons Volume 12 2019 10.1093/biohorizons/hzy013

Review article

Illuminating the secrets of crystals: microcrystal electron diffraction in structural biology

Rob Barringer*

C.101, Biomedical Sciences, University walk, University of Bristol, United Kingdom, BS8 1TD

***Corresponding author: Centre for structure Biology, Sir Ernst Chain Building, Imperial College London, United Kingdom, SW7 2AZ** Email: r.barringer@bristol.ac.uk

Supervisor: Professor Thomas Meier, Room 501, Sir Ernst Chain building, imperial college London, South Kensington, London, United Kingdom, SW7 2AZ.

X-ray crystallography (XRC) has visualised biological macromolecules in exquisite detail for over 50 years, relying on a combination of mathematical principles to offer insight into atomic structures. Crystals can diffract various electromagnetic waves aside from the conventional X-ray, offering an alternative approach to crystallographic structural analysis. Microcrystal electron diffraction (MicroED) illuminates crystals with electron waves instead of X-rays. Two specialised groups have demonstrated that MicroED can give high-resolution (often atomic) data, and now appears to be developing into a powerful alternative method to XRC or electron microscopy of macromolecules. How MicroED compares to XRC will be key to assessing it as a stand-alone crystallographic technique. This review presents a critical analysis of MicroED, with comments on theoretical and practical aspects and suggestions of further work and development.

Key words: MicroED, crystallography, structural biology, method development

Submitted on 23 July 2018; editorial decision on 23 November 2018

Introduction

Life is dependent on the ability of cells to perform a myriad of functions alone or in communities as tissues. When cellular processes falter, diseases can arise depending on the aberrant process. Understanding these processes is therefore essential to understanding the cellular basis of disease pathology. Cellular functions depend on proteins, of which there are likely over 19 000 in humans (Ezkurdia *et al.*, 2014), each with unique functions and interacting with various biomolecules (Rolland *et al.*, 2014). Proteins act as nano-scale cellular 'tools' with functions that are intimately linked to their unique structure; the role that protein architecture plays in biomolecular interactions has a long history, most commonly typified in the mind of the public by the 'lock-and-key' hypothesis (Koshland, 1994). Since proteins are incredibly small (for example haemoglobin has a diameter of ~1/200 000th of a mm) (Erickson, 2009), structural studies require the use of complex experimental methods, denoting the field of 'structural biology'. There are three main methods used to assess protein structure: Electron microscopy (EM), Nuclear magnetic resonance, and X-ray crystallography (XRC) (Curry, 2015), with XRC having the richest history of the three (Wilkins, 2013). This review focusses on a new crystallographic method (microcrystal electron diffraction; MicroED) that uses electrons instead of X-rays, outlining a brief history of both and then presenting a critical comparison of theoretical and practical aspects.

A short history of crystallography

XRC has been the primary macromolecular structural method for over 50 years (Jaskolski, Dauter and Wlodawer, 2014). The theory of the method is simple: a pure crystal containing exquisitely ordered repeating units of identical molecules are placed in the path of an X-ray beam, which is scattered by the molecules within the crystal to produce a

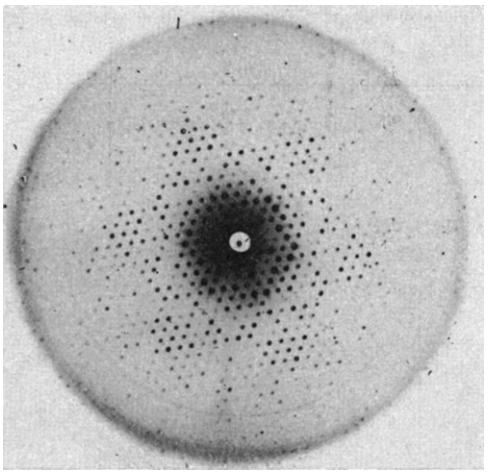

Figure 1. The X-ray diffraction pattern of glycine modified mono-acetoacetyl insulin. Protein crystals give unique diffraction patterns due to the atomic arrangement of the protein (i.e. the structure of the macromolecule). Each crystal has a characteristic diffraction pattern that can be analysed to determine the atomic structure of the crystallised molecule. Above is the diffraction pattern of glycine modified mono-acetoacetyl insulin, which presents a symmetrical six-sided pattern. This research was originally published in the *Biochemical Journal* (Lindsay and Shall 1969), reprinted with permission.

constellation-style pattern (Fig. 1). While beautiful to the naked eye, the symmetry and 'brightness' of each spot of the 'diffraction pattern' contains crucial structural information about the molecules that scattered the X-rays (Sweet, 1985). Crystallographers use the information from diffraction patterns to elucidate the atomic structures of biomolecules, allowing us to gain an atomistic perspective of nature's tools. X-rays were first used in crystallography by Max von Laue, who hypothesised that X-ray wavelengths are short enough to be diffracted by atoms within a 3-dimensional crystal (Eckert, 2012). Incoming X-rays excite the electrons surrounding atoms of the protein molecules in the crystal, and the X-ray energy is subsequently redistributed in all directions as a wave. In certain directions, the diffracted X-rays of each identical molecule interfere coherently (in phase) to produce observable diffraction 'spots'. The Braggs showed that these angles of observation depend on the X-ray wavelength and the spacing between molecules in the crystal (Bragg and Bragg, 1913) and that the characteristic 'spotting' of diffraction patterns results from these two properties. The spots are observed because the scattered X-rays of the repeating molecules only amplify when they overlap with each other *in phase*, which occurs at discrete angles relative to the crystal to create a 'reciprocal lattice' of spotting. The brightness of each spot results from the cumulative X-ray waves scattered from every atom of every molecule, overlapping in unique phases at each angle to give an average phase that produces a characteristic spot intensity (i.e. spot 'brightness'). Each crystal therefore gives a unique diffraction pattern (Fig. 1), which is measured and used to determine the exact atomic positions of the molecules within the crystal to solve the atomic structure of the molecules.

Electron crystallography

X-rays interfere weakly with matter compared to electrons, so XRC requires large volumes of matter create sufficient X-ray diffraction before the destructive effects of the radiation degrade the crystal (Henderson, 1995). The damaging effects are because X-rays deposit 1333× more energy than electrons into the crystal per elastic scattering (ES) event (single scattering of a wave without loss of amplitude or phase) (80 keV vs 60 eV per ES respectively) but electrons interact more frequently, degrading crystals very quickly (Glaeser, 1971). To accommodate for this challenge, 2-dimensional electron crystallography (2DEC) was developed in the 1970s, using thin crystals that reduce electron interaction, thereby reducing noise and enabling crystal illumination with electrons. The technique successfully determined the structure of purple membrane protein (today known as the light-driven proton pump 'bacteriorhodopsin') and the enzyme catalase (Henderson and Unwin, 1975; Unwin and Henderson, 1975) and had the unique ability to form 2-dimensional crystals of proteins within a lipid bilayer (an important property of native membrane proteins, Gonen *et al.*, 2005; Andrews, Reichow and Gonen, 2008; Wisedchaisri, Reichow and Gonen, 2011). During the late 2000s, Jan Pieter Abrahams applied electron crystallography to cryogenic 3-dimensional macromolecular crystals to create a method termed 3-dimensional electron crystallography (3DEC), gaining single diffraction patterns from microcrystals of Lysozyme which had previously proved difficult to achieve (Georgieva *et al.*, 2007b). As it turned out, the individual diffraction patterns provided a challenge as the relative orientation of the crystal lattice for each pattern was unknown, so merging diffraction data from multiple crystals was difficult. Data processing methods were then developed (Jiang *et al.*, 2009) (Abrahams, 2010), before improved detectors yielded better signal-to-noise ratios (SNR) (Nederlof *et al.*, 2011). Reducing electron dosage (to 0.1 e^{-} $Å^{-2}$ s^{-1}) prevented degradation and acquired more diffraction patterns per crystal (Nederlof *et al.*, 2013), allowing patterns to be orientated.

The history of MicroED

Low dose electron beams using 3D microcrystals

MicroED (hereon used as a catch-all term for MicroED/3DEC) was developed by Tamir Gonen, using cryogenically treated 3D Lysozyme microcrystals of 2 µm × 2 µm × 0.5 µm to demonstrate proof of concept (Fig. 2) (Shi *et al.*, 2013). As with Abrahams, Gonen found that after $9e^{-}/Å^{2}$ the diffraction patterns deteriorated, thus by using ~0.5 $µM^{3}$ microcrystals and a 0.01e^{-} $Å^{-2}$ s^{-1} dosage over 10 second exposures per angle, they collected 90 diffraction patterns per crystal, three times more than (Nederlof *et al.*, 2013). A wavelength of 0.025 Å (with a 200 kV acceleration current) was used, significantly shorter than typical XRC wavelengths (~1 Å).

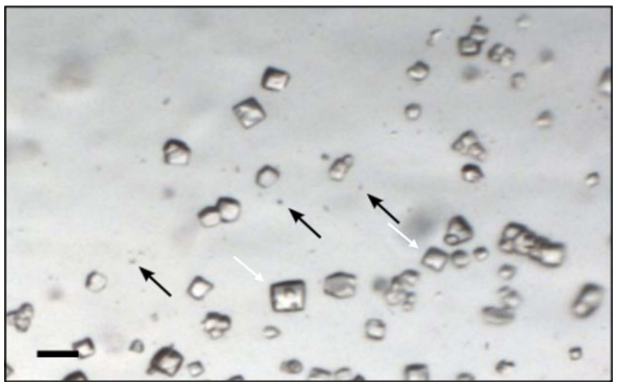

Figure 2. A comparison of Lysozyme microcrystals for MicroED (black arrows) and large crystals for XRC (white arrows). Microcrystals are ~6 orders of magnitude smaller than XRC crystals. Microcrystals are ~0.5–1 μM thick with ~55 × 106 unit cells. Crystals are screened by initial illumination to assess diffraction quality. For discussions on volume limitations, see optimal crystal sizes. Scale bar is 50 μM. This research was originally published in *eLIFE* (Shi *et al.*, 2013). Image has undergone a minor edit to include white arrows.

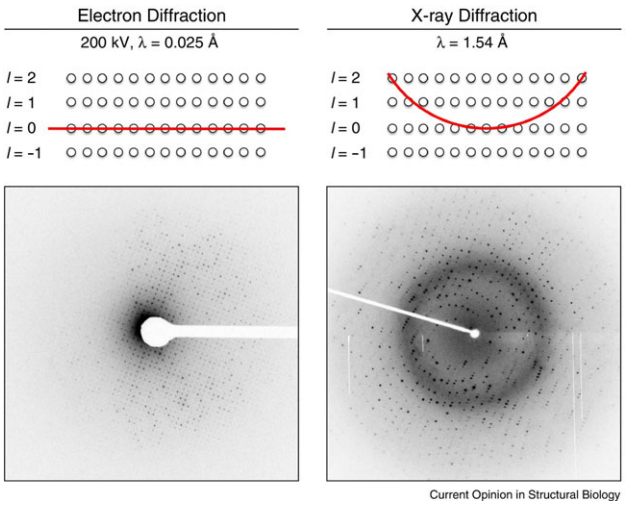

Figure 3. Illumination using electrons creates slices (left) through reciprocal space instead of lunes typically observed in XRC (right). Diffraction patterns of lysozyme are shown. The images show that at an angle perpendicular to a crystal axis, every reciprocal lattice point within the plane was observed using electron sources (with a complete absence of lune formation), while the XRC experiment demonstrated circular lunes. This research was originally published in *Current Opinion in Structural Biology* (Nannenga and Gonen, 2014), published under the CC-BY-NC-ND license.

Consequently, the Bragg angles are more acute and show more diffraction spots in a single illumination; the Ewald sphere (a mathematical tool to determine accessible reciprocal lattice points from a single illumination) is so large that it's surface is virtually flat, producing slices through reciprocal space instead of the lunes seen in XRC, sampling more lattice points (Fig. 3, Nannenga and Gonen, 2014). Crystals were rotated 1° between illuminations by tilting the specimen stage, with each spot averaging 34 observations from multiple angles. Since the slices through reciprocal space do not intersect spots perfectly, true spot intensities were difficult to derive, leading to loss of intensity data. Crude intensity approximations were made by assuming that the highest spot intensity represented the 'true' value. Using this initial approach, the Lysozyme structure was solved to 2.9 Å, using molecular replacement (MR, a technique that derives phase information from prior experiments of the same molecule) (Cipriani *et al.*, 2012).

Continuous crystal rotation in MicroED

The Gonen group introduced 'continuous rotation' MicroED; uninterrupted observation of diffraction data during continual crystal rotation, with frame rates of 4 s/frame with 0.09°/s rotation (Nannenga *et al.*, 2014b). The subsequent lysozyme pattern compared better with XRC diffraction data than static-MicroED (2.5 vs 2.9 Å respectively, Fig. 4), likely because (a) rotation allows proper intersection of reciprocal lattice points with the Ewald sphere and (b) rotation reduces beam contact time, lessening inelastic-scattering (IES, where incident electrons are deflected by atomic electrons and impart some energy into the crystal) and multiple elastic-scattering (MES, where electrons elastically scatter multiple times), both of which interfere with diffracting waves to create noise in data (see 'MicroED and XRC' section). This matched previous observations that rotation reduces IES/MES contribution to diffraction data (Georgieva *et al.*, 2007a; Gjonnes *et al.*, 1998; Gemmi *et al.*, 2003), resulting in continuous rotation becoming standard in MicroED. A suggestion that larger unit cells (the repeating unit of molecules throughout the crystal) and lower symmetry (the orientation of proteins within the unit cell) of the static vs CR Lysozyme structure may have increased noise due to lower protein/solvent ratios, increasing solvent contribution to the diffraction pattern and lowering resolution (see 'Optimal crystal sizes' section). Further MicroED work used XRC software to generate a Catalase structure to 3.2 Å (Nannenga *et al.*, 2014b).

The resolution breakthrough

More MicroED macromolecular structures were solved, leading to protocols outlining data collection and analysis (Hattne *et al.*, 2015, 2016; Shi *et al.*, 2016) including microcrystal acquisition from macro-crystals (de la Cruz *et al.*, 2017). Two breakthrough studies using MicroED without complementary X-ray MR data were published: the structure of α-synuclein gained by MR that utilised β-strand motifs as a search model for this simple protein (Rodriguez *et al.*, 2015) and an Sup35 amyloid core component (GNNQQNY, a hepta-peptide) (Sawaya *et al.*, 2016). This marked a turning point for MicroED; solving protein structures without prior XRC data (*ab initio*), an achievement previously applied only to organic compounds (van Genderen *et al.*, 2016). The first novel macromolecule structure, TGF-βm; TβRII, was published soon after (de la Cruz *et al.*, 2017). More than 17 structures

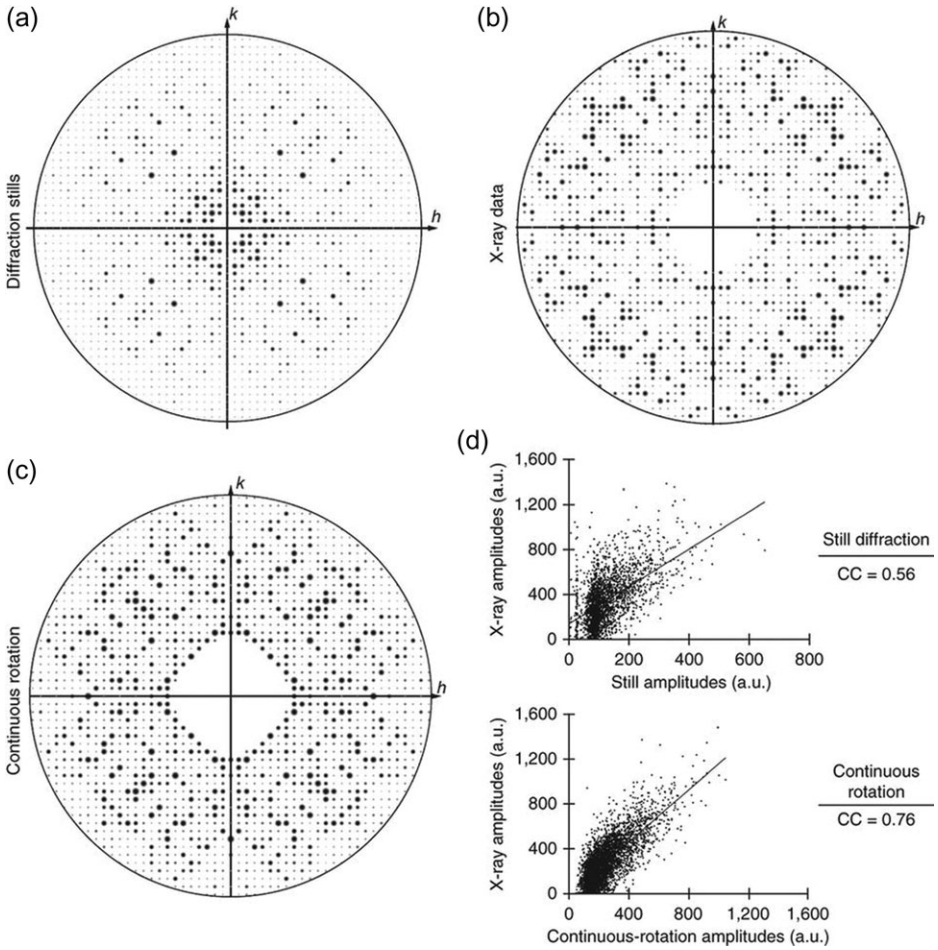

Figure 4. Lysozyme diffraction data of CR MicroED, static-frame MicroED and XRC experiments. The (001) diffraction plane of lysozyme using continuous rotation MicroED (**c**), static-MicroED (**a**) and XRC (**b**) are shown. Continuous rotation MicroED shows the best agreement with the XRC diffraction pattern. The Pearson correlation coefficients shown in (**d**) were 0.76 between continuous rotation MicroED (c) and X-ray data (b), vs 0.56 for static-frame MicroED (a) and X-ray data (b). Reprinted by permission from Springer Nature: Springer Nature Methods (Nannenga *et al.*, 2014b).

have been solved by MicroED (Rodriguez, Eisenberg and Gonen, 2017), with subsequent structures appearing in literature on a semi-regular basis (Krotee *et al.*, 2017; Gallagher-Jones *et al.*, 2018; Guenther *et al.*, 2018), many within the sub-angstrom range such as the fused in sarcoma (FUS) protein amyloid forming core to 0.73 Å (Luo *et al.*, 2018). Recent reviews highlight MicroED's history and future improvements (Rodriguez, Eisenberg and Gonen, 2017) and mathematical and theoretical principles (Clabbers and Abrahams, 2018).

Technical requirements and method procedure

Can the typical EM department implement MicroED? A comprehensive guide with a trouble-shooting section was recently outlined (Nannenga and Gonen, 2018), explaining that standard equipment used in single particle analysis/typical EM suites (EM, tilting stage, carbon grids and liquid ethane vitrification) are sufficient for MicroED. MicroED requires a high frame rate camera fast enough to capture individual reflections and prevent spot overlap, and high-speed detectors to minimise between-frame readout times, such as direct electron detectors (as used previously by the Abrahams group, van Genderen *et al.*, 2016). A previous guide was also outlined explaining how to make a device to control continuous crystal tilt (Shi *et al.*, 2016) and which equipment, data acquisition and processing methods are necessary. Briefly, the process involves crystallisation and microcrystal identification, EM/stage height/tilt calibration and setting up data collection processes. Data can now be processed and refined using standard XRC software, and structural models can be built using COOT, as outlined by Hattne *et al.*, 2015. Thus, aside from an appropriate camera, MicroED is readily available to any department equipped for single particle analysis, with supporting protocols and guides to aid researchers.

MicroED and XRC

To critically assess the efficacy and technical requirements of MicroED, it is useful to compare it with the current leading methods in XRC. Synchrotron facilities and X-ray free-electron lasers (XFELs) generate continuous or pulsed X-rays useful for the determination of high-resolution XRC structures. Fortunately, MicroED and XFELs have acquired multiple lysozyme structures (a molecule often used when developing and validating crystallographic methods), which offers a useful means of comparison. XFELs have yielded a 0.65 Å lysozyme structure (Wang *et al.*, 2007) compared to the 1.8 Å structure from MicroED (de la Cruz *et al.*, 2017), demonstrating that XRC techniques are currently still superior to MicroED for macromolecular crystallography. The difference in resolution may be partially due to MicroED's unique challenges with relation to the manner in which electrons/matter interactions give rise to IES and MES. Complications arising from IES for XRC/MicroED result from the addition of noise (as lower-energy deflected electrons interfere with diffracted waves) and crystal degradation. It is interesting to note that the ratio of IES/ES is much lower for electron interactions than X-ray interactions, implying that with further refinement, MicroED might have a lower IES-induced noise baseline than XRC. Conversely, the fact that electrons interact strongly with matter compared to X-rays creates significantly more scattering and more MES effects for MicroED, due to the weak scattering of X-rays by matter. In conventional XRC multiple scattering events are rare and presumed negligible, with individual diffraction spots derived mostly from single ES events (aka 'kinematical scattering') rather than more complicated multiple scattering events (aka 'dynamical scattering'). While dynamic scattering in rotational electron crystallography can be modelled (Oleynikov and Hovmöller, 2007), the complexity often obfuscates correct data interpretation, and should be reduced as much as possible. While MicroED might present with unique challenges, there are potentially some advantages that MicroED has over XRC. MicroED undoubtedly offers a cheaper and more accessible alternative to high-quality X-ray sources; many research institutes have an EM suite on site with short wait times, whereas synchrotron/XFEL facilities tend to only be found in regional hubs that typically require long wait times (Shi *et al.*, 2016). MicroED also requires a single or a few crystals compared to XFELs that require many, often taking time to produce. Crystallisation of macromolecules is often the critical time-consuming bottleneck in XRC studies. When crystallisation fails to produce large crystals (for synchrotron sources), such 'failed' conditions often produce MicroED-suitable microcrystals (Stevenson *et al.*, 2014, 2016). While previously regarded as a by-product of improper crystallisation, MicroED (and XFEL analysis) allows microcrystals to be useful for structural studies, allowing crystallographers to make use of more crystallisation conditions. MicroED methodology currently uses wavelengths of ~0.025 Å compared to ~0.55 Å in the highest resolution XRC structure, which is Cambrin (Schmidt *et al.*, 2011), with some considering the wavelength limit for XRC to be 0.5 Å (Jelsch *et al.*, 2000). With more development, one might consider it plausible that MicroED will surpass XRC. XRC currently achieves higher resolution than MicroED for macromolecules indicating that more refinement is required, but understanding how variables affect resolution may significantly close this gap (see 'Improvements for MicroED' section). One notable difference between XRC and MicroED lies in the 'phase problem'; while XRC routinely uses experimental methods to acquire phase information, such methods are challenging in electron crystallography, requiring a dependence on XRC MR data or *ab initio* phasing (see 'Overcoming the phase problem'). A better understanding of the critical MicroED parameters that affect resolution and development of phasing methods is required to improve resolution.

Challenges facing MicroED

Nannenga *et al.* (2014b) noted that large crystals may contribute more MES events, while separate work predicted that ≥0.1 µm thickness would give unusable data (Subramanian *et al.*, 2015). Surprisingly, proteinase K crystals of 0.1–1 µm thickness acquired good resolution when studied by whereby crystal disorder was suggested to explain the disparity between the experiment and predictions. Nonetheless, a negative correlation between crystal volume and resolution was observed; thick crystals absorbed electrons more frequently. This presents a problem; crystals must be large enough for observable ES, while minimising IES/MES. IES occurs three times more than ES to add noise, presenting an apparent challenge (Henderson, 1995). Phasing methods present another challenge; acquiring phases is challenging for X-ray (Taylor, 2003), electron (Dorset, 1997) and neutron crystallography (Hauptman and Langs, 2003). XRC overcomes this using Isomorphous Replacement (IR: heavy metal soaking of crystals to off-set phases and infer the original phases) and anomalous scattering (AS: whereby X-ray wavelength is altered to deposit energy into heavy metals which off-set phases to infer original phases) (Hendrickson and Ogata, 1997), but MicroED has not implemented IR/AS so far, an area of research that requires further investigation.

Improvements for MicroED

Rotation scope

MicroED typically uses a ±70° crystal tilt, which becomes problematic depending on crystal symmetry; most crystals present with space groups (notations denoting the repeating symmetry of proteins within unit cells) of $P2_12_12_1$ and $P2_1$ (Wukovitz and Yeates, 1995), giving unique diffraction spots over 180°. A ±70° tilt limits the accessible data to 140° from a single crystal (commonly known as the 'missing wedge' of EM, Bartesaghi *et al.*, 2008). A larger tilt might improve sampling, and efforts to create innovative solutions (such as those attempted by Barnard *et al.*, 1992) could be explored in the future.

Optimal crystal sizes

Crystals require sufficient volume to provide signal, while excessively large crystals generate significant MES/IES, prompting to suggest an upper limit of 500 µm for optimal diffraction. Microcrystals can be acquired from larger (>500 µm) crystals (de la Cruz *et al.*, 2017), but understanding the volume/resolution relationship is necessary. Interestingly, the highest resolution data currently derives from small unit cell crystals with complex symmetry (see Table 1), suggesting that perhaps the protein atomicity of a crystal (i.e. protein molecules per $Å^3$) or high solvent content (e.g. when protein atomicity is low) contributes to volume/resolution relationships. It is already known that solvents generate noise (Bragg and Perutz, 1952) (Fraser, MacRae and Suzuki, 1978), and are typically disordered and not uniformly oriented in crystals (Weichenberger *et al.*, 2015), which could increase noise when protein atomicity is low (since solvents occupy more volume). When reviewing MicroED structures (Table 1), an observable trend between protein atomicity and resolution appears (Fig. 5), however this compares structures over years from many laboratories, so variability is likely significant. Interestingly, Sawaya *et al.* (2016) analysed GNNQQNY in two different symmetries; the higher symmetry crystal gave better resolution, providing insight into atomicity/resolution relationships. Further research is essential to characterise the relationship between ES/MES/IES and crystal volume and atomicity.

Reducing electron dosage – crystal rotation speed

Electrons deposit less IES per ES than X-rays and less energy per IES, but interact more frequently with matter leading to quicker crystal degradation (Henderson, 1995). Electron dosage is kept below a critical threshold (Shi *et al.*, 2013) and continuous rotation reduces electron exposure to different crystal locations (Nannenga *et al.*, 2014a). Rotation speeds and frame rates are a compromise between adequate sampling of diffraction spots while preventing spot overlap (Hattne *et al.*, 2015).

A faster rotation with a shorter frame rate might reduce electron dosage while preventing spot overlap. Rotation speeds varied over experiments, from 0.1°/s (Vergara *et al.*, 2017) to 0.29°/s (de la Cruz *et al.*, 2017), but Table 1 shows that resolution vs rotation speed (Fig. 6) and frame scope (the angle covered by a single frame, Fig. 7) appears to show no apparent trend; different rotation speeds and frame scopes did not correlate with resolution; however, the data likely include significant inter-laboratory and inter-assay variability which may contribute to resolution quality. Indeed, the Gonen group attribute increased resolution over their three lysozyme structures to improved data collection and processing (Nannenga and Gonen, 2018). To date, no published work specifically dedicated to the effect of rotation speeds is available. Further research is required to probe rotation speed/frame rate contribution to diffraction patterns using identical crystals to control for other variables.

Reducing electron dosage – electron wavelength

The incident beam might be adjusted to reduce electron dosage; electrons with shorter wavelengths degrade crystals slower and improve longevity (Glaeser, 1971). While MicroED uses an electron wavelength of 0.025 Å, no work assessing wavelength effect on ES/IES/MES has been published. Electron exposure was assessed in proteinase K and GSNQNNF crystals; high-resolution spots degraded at the 0.025 Å wavelength (likely due to their typical low signal) with high-resolution data (<2.0 Å) being severely degraded at $\geq 3\ e^{-}\ Å^{-2}$ (Hattne *et al.*, 2018). At low doses electrons were absorbed and shielded atoms from proper ES, e.g. at $\geq 0.9\ e^{-}\ Å^{-2}$ disulphide bridges deteriorated and broke at $5.78\ e^{-}\ Å^{-2}$, while glutamate/aspartate residues lost carboxyl density at $\geq 2\ e^{-}\ Å^{-2}$, which was absent at $5\ e^{-}\ Å^{-2}$, meaning electron dosage contributes to structural quality and is an important element to control. Higher frequency electrons interact with matter less frequently (Birkhoff, 1958); further research could build on the work of Hattne *et al.* (2018) to determine whether shorter wavelengths might reduce interactions and IES/MES to improve resolution.

Overcoming the phase problem

2DEC IR techniques have been attempted, but shielding of metal nuclei by large electron clouds weakened IR interference (Ceska and Henderson, 1990), however some argued that heavy metal phase contributions can theoretically give sufficient information to solve phases (Burmester and Schröder, 1997). While MicroED has successfully used direct methods to process data (Sawaya *et al.*, 2016; de la Cruz *et al.*, 2017; Vergara *et al.*, 2017), these computational methods require resolution to be 1.2 Å or better, (aka 'Sheldricks rule', Sheldrick, 1990; Morris and Bricogne, 2003). Consequently, this method is currently limited to small molecules, which tend to give the highest resolution data (Taylor, 2010) as seen in the Sawaya *et al.* (2016) publication. Direct methods have been used on macromolecular data of ~2 Å in XRC by prospective MR using archetypal α-helices/β-sheets as search models, solving the structure of a previously unknown 111-residue protein (Rodriguez *et al.*, 2009). While useful, this may not be appropriate for macromolecules lacking sufficient α-helix and β-sheet structures. XRC also overcomes the phase problem using AS, requiring wave absorption by heavy atoms (Hendrickson and Ogata, 1997) an effect that electrons are believed to be capable of achieving (Burmester and Schröder, 1997). A breakthrough is needed in MicroED analogous to IR/AS to find dependable phasing methods for macromolecular crystals.

Improvements to equipment and data processing

The electron detector used in an EM plays a key part in detection and analysis of diffracted waves. Traditionally, EMs

Table 1. crystal rotation speed, frame rate and resolution

Molecule	Crystal rotation speed (°/s)	Frame rate (s/frame)	Rotation per frame (°)	Space group	Molecules per unit cell	Unit cell volume (Å^3)	Volume per molecule (Å^3)	Resolution (Å)	Reference
Proteinase K	0.090	4.0	0.360	$P4_32_12$	8	452 897	56 612	1.60	de la Cruz *et al.* (2017)
	0.089	5.1	0.454	$P4_32_12$	8	452 267	56 533	1.71	Hattne *et al.* (2018)
	0.090	4.0	0.360	*P43212*	8	457 776	57 222	1.75	Hattne *et al.* (2016)
Lysozyme	0.090	4.0	0.360	$P4_32_12$	8	215 821	26 978	1.80	de la Cruz *et al.* (2017)
	0.152	0.5	0.076	$P2_12_12$	4	228 046	57 012	2.11	Clabbers *et al.* (2017)
	0.450	2.0	0.900	$P2_12_12$	4	222 650	55 663	2.20	Xu *et al.* (2018)
	0.090	4.0	0.360	$P4_32_12$	8	212 691	26 586	2.50	Nannenga *et al.* (2014b)
	N/A	10.0	N/A	$P4_32_12$	8	219 373	27 422	2.90	Shi *et al.* (2013)
Catalase	0.09	6.0	0.540	$P2_12_12_1$	4	2 125 468	531 367	3.20	Nannenga *et al.* (2014a)
	0.75[a]	2.0[a]	1.500[a]	$P2_12_12_1$	4	2466 129	616 532	3.20	Yonekura and Maki-Yonekura (2016)
GNNQQNY	0.30	2.0	0.600	$P2_12_12_1$	4	4625	1156	1.05	Sawaya *et al.* (2016)
	0.30	2.0	0.600	$P2_1$	2	2726	1363	1.10	Sawaya *et al.* (2016)

The table shows MicroED experiments that used crystals of four proteins (proteinase K, lysozyme, catalase and the hepta-peptide GNNQQNY) under different crystal rotation speeds, frame rates, crystal unit cells and volumes, along with the resultant resolution of the final structures. References to relevant publications are given in the table. The relationship of resolution plotted against protein atomicity (density within the unit cell, defined as the volume per molecule), crystal rotation speed and frame scope (the total angle sampled by a single frame) are shown in Figs 5– 7, respectively.
[a]Note: for this catalase experiment, various frame rates and rotation speeds were used from 0.5 to 1.0° over 1–3 s per frame median values of these ranges are displayed in the table.

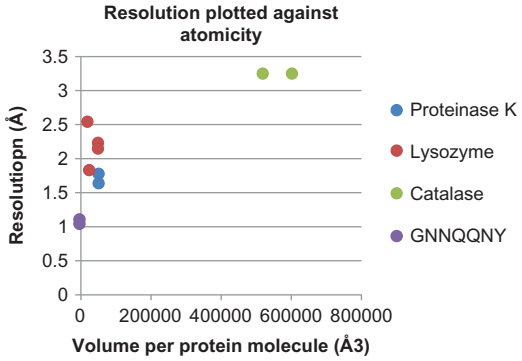

Figure 5. Resolution vs molecular crystal atomicity from MicroED structures of common proteins. MicroED structures of proteinase K (blue), lysozyme (red), catalase (green) and GNNQQNY hepta-peptide (purple) are plotted to correlate structure resolution to unit cell atomicity, i.e. volume per protein molecule. Crystals with higher symmetry and tighter packing have less volume per molecule and higher atomicity. More densely packed cells with higher atomicity give higher final structure resolution. All experimental information is derived from Table 1.

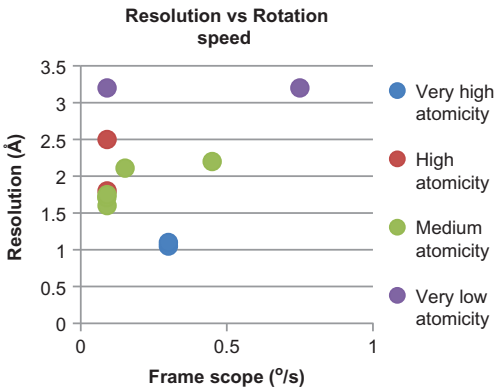

Figure 6. Resolution vs crystal rotation speed from MicroED structures of common proteins. The relationship between resolution and crystal rotation speed of all Table 1 molecules are shown above, colour coded for atomicity. Very high atomicity = 1000–1500 A^3/molecule, high atomicity = 25 000–30 000 A^3/molecule, medium atomicity = 55 000–60 000 A^3/molecule, Very low atomicity = 500 000–650 000 A^3/molecule.

have used two types of indirect detectors, Charge-Coupled Devices and Complementary Metal-Oxide-Semiconductors (CMOS). Both convert electrons to photons using a scintillator which are then detected by the sensor (a comparison is outlined in Allé *et al.*, 2016). The scintillation inherently introduces scatter, and bulky detectors can scatter photons laterally into neighbouring pixels, spreading the peak, making indirect detectors sub-optimal for electron crystallography (Faruqi, 2001). Hybrid detectors detect charge directly from electrons to prevent scintillator-associated scatter but due to the strong electron/matter interactions, they are easily damaged by the electron beam. Initial studies suggested that hybrid detectors may nonetheless perform better than indirect detectors to generate signal,

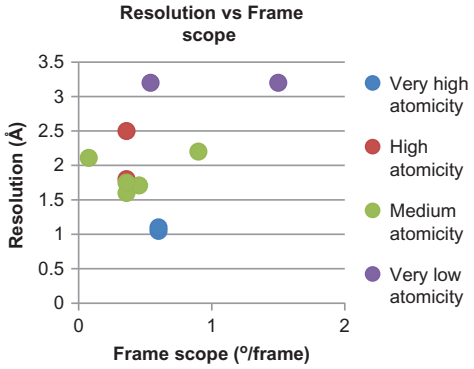

Figure 7. Resolution vs frame scope from MicroED structures of common proteins. The relationship between resolution and frame scope (angle sampled per camera frame) of all Table 1 molecules is shown above, colour coded for atomicity. Very high atomicity = 1000–1500 A^3/molecule, high atomicity = 25 000–30 000 A^3/molecule, medium atomicity = 55 000–60 000 A^3/molecule, very low atomicity = 50 0000–650 000 A^3/molecule.

provided that electron dosage was not sufficiently high to damage the detector (Clough, Moldovan and Kirkland, 2014). Tim Gruene's group is actively engaging in detector development (Nederlof *et al.*, 2013; van Genderen *et al.*, 2016; Clabbers *et al.*, 2017; Matheson *et al.*, 2017), recently demonstrating a novel ultrathin hybrid detector that samples smaller pixel areas and has shorter dead time between frames, reducing data loss from pixel-related overlap of intensities (Tinti *et al.*, 2018). The detector circuitry was specifically designed with beam resistance to reduce damage at energies of 100, 200 and 300 keV, while the Abrahams group applied new DIALS integration software (Clabbers *et al.*, 2018). The Gonen group noted that IES electrons may be filtered out of the diffraction data by using energy filters to remove IES (Nannenga *et al.*, 2014b) and improve SNR in line with other work (Yonekura, Maki-Yonekura and Namba, 2002; Leis *et al.*, 2009), but have seemingly not yet utilised this approach. Future innovation and development of equipment and data processing to improve SNR will greatly improve resolution, and energy filters may be an attractive option to remove IES from diffracting waves.

MicroED in the wider community

The worldwide structural biology community is increasingly using MicroED in structural studies and are taking an interest in the technical and theoretical aspects. One group published Lysozyme structures to 2.2 Å and commented on MicroED's main challenges, stating that crystal degradation and goniometric imperfections in crystal rotation are key challenges to overcome (Xu *et al.*, 2018). The first use of MicroED to study amyloid fibrils outside of the Gonen group was published recently, solving the (FUS) amyloid core to 0.73 Å (Luo *et al.*, 2018). Other groups are attempting to improve the technique and contribute to MicroED theory; some are researching and commenting on the relationship between microcrystal size

and diffraction spots (Williams *et al.*, 2017), while others suggest that maps generated from MicroED might be utilising sub-optimal MR methods as structure factors fail to take negative contributions from IES into account (Wang, 2017). While the technique is still very young, it is likely that the future will see a growing rate of MicroED structures being solved and published as the community begins to delve deeper into the intricacies of the method and develop it further. While the work of the Gonen and Abrahams group have undoubtedly contributed significantly to the technique, the wider community is now beginning to realise the potential that this novel method has within structural biology.

Conclusion

MicroED is an exciting crystallographic method utilising short wavelengths to offer better theoretical resolution limits than XRC, while simultaneously sampling more reciprocal space per illumination. While modern macromolecular EM work typically relies on single particle analysis without phasing methods or crystals (Orlova and Saibil, 2004), MicroED offers significantly higher resolution; a characteristic that makes crystallographic methods so popular (Wilkins, 2013). MicroED offers an affordable and accessible XRC alternative by utilising EMs commonly used in many structural laboratories with minor adjustments. Continuous rotation MicroED and XRC diffraction software have improved the method, but more work is required to characterise the effect of crystal volume, unit cell packing, electron wavelength, crystal rotation speed, frame rate capture, detector type and the use of energy filters on resolution. While MicroED works very well with small molecule crystals, its use on larger molecules lacks comparable resolution, likely due to solvent/protein ratios of large unit cells with low symmetry crystals creating noise. For high macromolecular resolution, MicroED depends on MR from XRC studies. To be a stand-alone technique, MicroED must develop phasing methods for macromolecular datasets. Computational methods have somewhat addressed this challenge at resolutions of 1.2 Å and 2.0 Å, but macromolecules typically give lower resolutions than 1.2 Å and even at 2.0 Å may not present sufficient secondary structures to utilise the phasing method, therefore phasing is particularly troublesome and must be addressed by developing innovative phasing methods. As it stands, MicroED is a powerful technique for small molecules, elucidating these structures in unprecedented detail and might perhaps be considered better than XRC in terms of resolution and practicality for this class of molecules. Further work and innovation will be essential for solving the MicroED phase problem, and given that the wider community is beginning to contribute to the technique, we may very well be on the cusp of producing the next series of breakthroughs for this impressive technique.

Author biography

Rob is now a BBSRC PhD candidate of Structural Biology at the University of Bristol, working with Dr Paul Race studying the structure and function of streptococcal adhesins. Rob has a keen interest in crystallography and wrote this article during his M.Res dissertation in Structural Molecular Biology at Imperial College London, after a BSc in Biomedical Science, MSc in Biomedical Blood Science at Keele University, and a PGCert in Protein Crystallography at Birkbeck. While working in clinical laboratories (transfusion and emergency medicine in Salisbury and Addenbrookes), Rob undertook the PGCert and decided to pursue a career in basic research. He then worked as a Tissue Acquisition Officer for the BCI, before working at UCB Celltech as an Associate Scientist in biopharmaceutical method development. In September 2017 he began his MRes, with the PhD beginning in September 2018. Post-PhD Rob would like to contribute to MicroED development within structural biology.

Acknowledgements

I would like to thank my supervisor, Thomas Meier, for his guidance and feedback. I would like to thank Morgan Beeby for his invaluable insight concerning electron microscopy and electron/matter interactions. I would also like to thank Jose Rodriguez for his fruitful correspondence concerning MicroED, current research and future directions for the method.

References

Abrahams, J. P. (2010) The strong phase object approximation may allow extending crystallographic phases of dynamical electron diffraction patterns of 3D protein nano-crystals, *Zeitschrift fur Kristallographie-Crystalline Materials*, 225, 67–76.

Allé, P., Wenger, E., Dahaoui, S. et al. (2016) Comparison of CCD, CMOS and hybrid pixel X-ray detectors: detection principle and data quality, *Physica Scripta*, 91, 063001.

Andrews, S., Reichow, S. L. and Gonen, T. (2008) Electron crystallography of aquaporins, *IUBMB Life*, 60, 430–436.

Barnard, D. P., Turner, J. N., Frank, J. et al. (1992) A 360° single-axis tilt stage for the high-voltage electron microscope, *Journal of Microscopy*, 167, 39–48.

Bartesaghi, A., Sprechmann, P., Liu, J. et al. (2008) Classification and 3D averaging with missing wedge correction in biological electron tomography, *Journal of Structural Biology*, 162 (3), 436–450.

Birkhoff, R. D. (1958) The passage of fast electrons through matter, in Flügge S. (ed), *Corpuscles and Radiation in Matter II*, 1st edition, Springer, Berlin/Heidelberg, pp. 53–138.

Bragg, W. H. and Bragg, W. L. (1913) The reflection of X-rays by crystals, *Proceedings of the Royal Society London*, 88, 428–438.

Bragg, W. H. and Perutz, M. F. (1952) The external form of the haemoglobin molecule. I, *Acta Crystallographica*, 5, 277–283.

Burmester, C. and Schröder, R. R. (1997) Solving the phase problem in protein electron crystallography: multiple isomorphous replacement and

anomalous dispersion as alternatives to imaging, *Scanning Microscopy*, 11, 323–334.

Ceska, T. A. and Henderson, R. (1990) Analysis of high-resolution electron diffraction patterns from purple membrane labelled with heavy-atoms, *Journal of Molecular Biology*, 213, 539–560.

Cipriani, F., Roewer, M., Landret, C. et al. (2012) CrystalDirect: a new method for automated crystal harvesting based on laser-induced photoablation of thin films, *Acta Crystallographica Section D—Biological Crystallography*, 68, 1393–1399.

Clabbers, M. T. B. and Abrahams, J. P. (2018) Electron diffraction and three-dimensional crystallography for structural biology, *Crystallography Reviews*, 24 (3), 176–204.

Clabbers, M. T. B., Gruene, T., Parkhurst, J. M. et al. (2018) Electron diffraction data processing with DIALS, *Acta Crystallographica section D—Structural Biology*, 74, 506–518.

Clabbers, M. T. B., van Genderen, E., Wan, W. et al. (2017) Protein structure determination by electron diffraction using a single three-dimensional nanocrystal, *Acta Crystallographica Section D—Structural Biology*, 73, 738–748.

Clough, R. N., Moldovan, G. and Kirkland, A. I. (2014) Direct detectors for electron microscopy, *Journal of Physics Conference Series*, 522, 012046.

Curry, S. (2015) Structural biology: a century-long journey into an unseen world, *Interdisciplinary Science Reviews*, 40, 308–328.

de la Cruz, M. J., Hattne, J., Shi, D. et al. (2017) Atomic-resolution structures from fragmented protein crystals with the cryoEM method MicroED, *Nature Methods*, 14 (4), 399–402.

Dorset, D. L. (1997) Direct phase determination in protein electron crystallography: the pseudo-atom approximation, *Proceedings of the National Academy of Sciences of the United States of America*, 94, 1791–1794.

Eckert, M. (2012) Max von Laue and the discovery of X-ray diffraction in 1912, *Annalen Der Physik*, 524 (5), A85.

Erickson, H. P. (2009) size and shape of protein molecules at the nanometer level determined by sedimentation, gel filtration, and electron microscopy, *Biological Procedures Online*, 11, 32–51.

Ezkurdia, I., Juan, D., Manuel Rodriguez, J. et al. (2014) Multiple evidence strands suggest that there may be as few as 19 000 human protein-coding genes, *Human Molecular Genetics*, 23, 5866–5878.

Faruqi, A. R. (2001) Prospects for hybrid pixel detectors in electron crystallography, *Nuclear Instruments and Methods in Physics Research A*, 466, 146–154.

Fraser, R. D. B., MacRae, T. P. and Suzuki, E. (1978) An improved method for calculating the contribution of solvent to the X-ray diffraction pattern of biological molecules, *Journal of Applied Crystallography*, 11, 693–694.

Gallagher-Jones, M., Glynn, C., Boyer, D. R. et al. (2018) Sub-angstrom cryo-EM structure of a prion protofibril reveals a polar clasp, *Nature Structural & Molecular Biology*, 25 (2), 131–134.

Gemmi, M., Zou, X., Hovmöller, S. et al. (2003) Structure of Ti2P solved by three-dimensional electron diffraction data collected with the precession technique and high-resolution electron microscopy, *Acta Crystallographica A—Foundations and Advances*, 59, 117–126.

Georgieva, D., Abrahams, J. P., Zandbergen, H. et al. (2007a) Solving ab-initio protein and nanostructures with precession electron diffraction, *Microscopy and Microanalysis*, 13, 952–953.

Georgieva, D. G., Kuil, M. E., Oosterkamp, T. H. et al. (2007b) Heterogeneous nucleation of three-dimensional protein nanocrystals, *Acta Crystallographica Section D—Biological Crystallography*, 63, 564–570.

Gjonnes, J., Hansen, V., Berg, B. S. et al. (1998) Structure model for the phase almfe derived from three-dimensional electron diffraction intensity data collected by a precession technique. comparison with convergent-beam diffraction, *Acta Crystallographica Section A-Foundations and Advances*, 54, 306–319.

Glaeser, R. M. (1971) Limitations to significant information in biological electron microscopy as a result of radiation damage, *Journal of Ultrastructure Research*, 36, 466–482.

Gonen, T., Cheng, Y. F., Sliz, P. et al. (2005) Lipid-protein interactions in double-layered two-dimensional AQP0 crystals, *Nature*, 438, 633–638.

Guenther, E. L., Ge, P., Trinh, H. et al. (2018) Atomic-level evidence for packing and positional amyloid polymorphism by segment from TDP-43 RRM2, *Nature Structural & Molecular Biology*, 25, 311–319.

Hattne, J., Reyes, F. E., Nannenga, B. L. et al. (2015) MicroED data collection and processing, *Acta Crystallographica A-Foundation and Advances*, 71, 353–360.

Hattne, J., Shi, D., de la Cruz, M. J. et al. (2016) Modeling truncated pixel values of faint reflections in MicroED images, *Journal of Applied Crystallography*, 49, 1029–1034.

Hattne, J., Shi, D., Glynn, C. et al. (2018) Analysis of global and site-specific radiation damage in cryo-EM, *Structure (London, England : 1993)*, 26, 759–766.

Hauptman, H. A. and Langs, D. A. (2003) The phase problem in neutron crystallography, *Acta Crystallographica Section A*, 59, 250–254.

Henderson, R. (1995) The potential and limitations of neutrons, electrons and X-rays for atomic-resolution microscopy of unstained biological molecules, *Quarterly Reviews of Biophysics*, 28, 171–193.

Henderson, R. and Unwin, P. (1975) 3-Dimensional model of purple membrane obtained by electron-microscopy, *Nature*, 257, 28–32.

Hendrickson, W. A. and Ogata, C. M. (1997) Phase determination from multiwavelength anomalous diffraction measurements, *Methods in Enzymology*, 276, 494–523.

Hughes, M. P., Sawaya, M. R., Goldschmidt, L. et al. (2017) Low-complexity domains adhere by reversible amyloid-like interactions between kinked β-sheets. *bioRxiv* (in press) doi: 10:10:/153817

Jaskolski, M., Dauter, Z. and Wlodawer, A. (2014) A brief history of macromolecular crystallography, illustrated by a family tree and its Nobel fruits, *FEBS*, 281, 3985–4009.

Jelsch, C., Teeter, M. M., Lamzin, V. et al. (2000) Accurate protein crystallography at ultra-high resolution: valence electron distribution in

crambin, *Proceedings of the National Academy of Sciences of the United States of America*, 97, 3171–3176.

Jiang, L., Georgieva, D., Zandbergen, H. W. et al. (2009) Unit-cell determination from randomly oriented electron-diffraction patterns, *Acta Crystallographica Section D—Biological Crystallography*, 65, 625–632.

Koshland, D. E. (1994) The key-lock theory and the induced fit theory, *Angewandte Chemie-International Edition*, 33, 2375–2378.

Krotee, P., Rodriguez, J. A., Sawaya, M. R. et al. (2017) Atomic structures of fibrillar segments of hIAPP suggest tightly mated beta-sheets are important or cytotoxicity, *Elife*, 6, e19273.

Leis, A., Rockel, B., Andrees, L. et al. (2009) Visualizing cells at the nanoscale, *Trends in Biochemical Sciences*, 34, 60–70.

Lindsay, D. G. and Shall, S. (1969) Acetoacetylation of insulin, *Biochemical Journal*, 115, 587–595. doi:10.1042/bj1150587 the figure used in Figure 1 was original published by Portland Press under the STM permission guidelines (https://www.stm-assoc.org/copyright-legal-affairs/permissions/permissions-guidelines/), and request has been granted to use the figure.

Luo, F., Gui, X., Zhou, H. et al. (2018) Atomic structures of FUS LC domain segments reveal bases for reversible amyloid fibril formation, *Nature Structural & Molecular Biology*, 25, 341–346.

Matheson, J., Moldovan, G., Kirkland, A. et al. (2017) Testing and comparison of imaging detectors for electrons in the energy range 10–20 keV, *Journal of Instrumentation*, 12, C11016. International Conference on Position Sensitive Detectors.

Morris, R. J. and Bricogne, G. (2003) Sheldrick's 1.2 angstrom rule and beyond, *Acta Crystallographica Section D—Biological Crystallography*, 59, 615–617.

Nannenga, B. L. and Gonen, T. (2014) Protein structure determination by MicroED, *Current Opinion in Structural Biology*, 27, 24–31. The figure used in **Figure 3** was originally published by Elsevier and request has been granted to use the figure by the Copyright Clearance Centre (license 4367131293431).

Nannenga, B. L. and Gonen, T. (2018) MicroED: a versatile cryoEM method for structure determination, *Emerging Topics in Life Sciences*, 2, 1–8.

Nannenga, B. L., Shi, D., Hattne, J. et al. (2014a) Structure of catalase determined by MicroED, *Elife*, 3, e03600.

Nannenga, B. L., Shi, D., Leslie, A. G. W. et al. (2014b) High-resolution structure determination by continuous-rotation data collection in MicroED, *Nature Methods*, 11, 927–930. The figure used in **Figure 4** was original published by Springer Nature and request has been granted to use the figure by the Copyright Clearance Centre (license 4367140499674).

Nederlof, I., Georgieva, D. and Abrahams, J. P. (2011) Electron diffraction of submicron 3D protein crystals, *Acta Crystallographica Section A-Foundation and Advances*, 67, C228.

Nederlof, I., van Genderen, E., Li, Y. et al. (2013) A Medipix quantum area detector allows rotation electron diffraction data collection from submicrometre three-dimensional protein crystals, *Acta Crystallographica Section D—Biological Crystallography*, 69, 1223–1230.

Oleynikov, P. and Hovmöller, S. (2007) Precession electron diffraction: observed and calculated intensities, *Ultramicroscopy*, 107, 523–533.

Orlova, E. V. and Saibil, H. R. (2004) Structure determination of macromolecular assemblies by single-particle analysis of cryo-electron micrographs, *Current Opinion in Structural Biology*, 14, 584–590.

Rodriguez, J. A., Eisenberg, D. S. and Gonen, T. (2017) Taking the measure of MicroED, *Current Opinion in Structural Biology*, 46, 79–86.

Rodriguez, D. D., Grosse, C., Himmel, S. et al. (2009) Crystallographic ab initio protein structure solution below atomic resolution, *Nature Methods*, 6, U39.

Rodriguez, J. A., Ivanova, M. I., Sawaya, M. R. et al. (2015) Structure of the toxic core of alpha-synuclein from invisible crystals, *Nature*, 525, 486–490.

Rolland, T., Tasan, M., Charloteaux, B. et al. (2014) A proteome-scale map of the human interactome network, *Cell*, 159, 1212–1226.

Sawaya, M. R., Rodriguez, J., Cascio, D. et al. (2016) Ab initio structure determination from prion nanocrystals at atomic resolution by MicroED, *Proceedings of the National Academy of Sciences of the United States of America*, 113, 11232–11236.

Schmidt, A., Teeter, M., Weckert, E. et al. (2011) Crystal structure of small protein crambin at 0.48 Å resolution, *Acta Crystallographica Section F- Structural Biology Communications*, 67, 424–428.

Sheldrick, G. M. (1990) Phase annealing in Shelx-90—direct methods for larger structures, *Acta Crystallographica Section A*, 46, 467–473.

Shi, D., Nannenga, B. L., de la Cruz, M. J. et al. (2016) The collection of MicroED data for macromolecular crystallography, *Nature Protocols*, 11, 895–904.

Shi, D., Nannenga, B. L., Iadanza, M. G. et al. (2013) Three-dimensional electron crystallography of protein microcrystals, *Elife*, 2, e01345. The figure used in **Figure 2** was original published under the Creative Commons Attribution 3.0 Unported (CC BY 3.0) license (https://creativecommons.org/licenses/by/3.0/), and request has been granted to use the figure.

Stevenson, H. P., Lin, G., Barnes, C. O. et al. (2016) Transmission electron microscopy for the evaluation and optimization of crystal growth, *Acta Crystallographica Section D—Structural Biology*, 72, 603–615.

Stevenson, H. P., Makhov, A. M., Calero, M. et al. (2014) Use of transmission electron microscopy to identify nanocrystals of challenging protein targets, *Proceedings of the National Academy of Sciences of the United States of America*, 111, 8470–8475.

Subramanian, G., Basu, S., Liu, H. et al. (2015) Solving protein nanocrystals by cryo-EM diffraction: Multiple scattering artifacts, *Ultramicroscopy*, 148, 87–93.

Sweet, R. M. (1985) Introduction to Crystallography, *Methods in Enzymology*, 114, 19–46.

Taylor, G. (2003) The phase problem, *Acta Crystallographica Section D—Biological Crystallography*, 59, 1881–1890.

Taylor, G. L. (2010) Introduction to phasing, *Acta Crystallographica Section D—Biological Crystallography*, 66, 325–338.

Tinti, G., Frojdh, E., van Genderen, E. et al. (2018) Electron crystallography with the EIGER detector, *IUCRJ*, 5, 190–199.

Unwin, P. and Henderson, R. (1975) Molecular-structure determination by electron-microscopy of unstained crystalline specimens, *Journal of Molecular Biology*, 94, 425–440.

van Genderen, E., Clabbers, M. T. B., Das, P. P. et al. (2016) Ab initio structure determination of nanocrystals of organic pharmaceutical compounds by electron diffraction at room temperature using a Timepix quantum area direct electron detector, *Acta Crystallographica A-Foundation and Advances*, 72, 236–242.

Vergara, S., Lukes, D. A., Martynowycz, M. W. et al. (2017) MicroED structure of Au-146(p-MBA)(57) at subatomic resolution reveals a twinned FCC cluster , *Journal of Physical Chemistry Letters*, 8, 5523–5530.

Wang, J. (2017) On the appearance of carboxylates in electrostatic potential maps, *Protein Science*, 26, 396–402.

Wang, J., Dauter, M., Alkire, R. et al. (2007) Triclinic lysozyme at 0.65 Å resolution, *Acta Crystallographica Section D—Biological Crystallography*, 63, 1254–1268.

Weichenberger, C. X., Afonine, P. V., Kantardjieff, K. et al. (2015) The solvent component of macromolecular crystals, *Acta Crystallographica Section D—Biological Crystallography*, 71, 1023–1038.

Wilkins, S. W. (2013) Celebrating 100 years of X-ray crystallography, *Acta Crystallographica Section A*, 69, 1–4.

Williams, S. R., Dilanian, R. A., Quiney, H. M. et al. (2017) Analysis of diffracted intensities from finite protein crystals with incomplete unit cells, *Crystals*, 7, 220.

Wisedchaisri, G., Reichow, S. L. and Gonen, T. (2011) Advances in structural and functional analysis of membrane proteins by electron crystallography, *Structure (London, England : 1993)*, 19, 1381–1393.

Wukovitz, S. W. and Yeates, T. O. (1995) Why protein crystals favor some space-groups over others, *Nature Structural Biology*, 2, 1062–1067.

Xu, H., Lebrette, H., Yang, T. et al. (2018) A rare lysozyme crystal form solved using highly redundant multiple electron diffraction datasets from micron-sized crystals, *Structure (London, England : 1993)*, 26, 667–675.

Yonekura, K. and Maki-Yonekura, M. (2016) Refinement of cryo-EM structures using scattering factors of charged atoms, *Journal of Applied Crystallography*, 49, 1517–1523.

Yonekura, K., Maki-Yonekura, S. and Namba, K. (2002) Quantitative comparison of zero-loss and conventional electron diffraction from two-dimensional and thin three-dimensional protein crystals, *Biophysical Journal*, 82, 2784–2797.